Structural Studies on the Reaction of Isopenicillin N Synthase with the Truncated Substrate Analogues δ-(L-α-aminoadipoyl)-L-cysteinyl-glycine and δ-(L-α-aminoadipoyl)-L-cysteinyl-D-alanine[†,‡]

Alexandra J. Long,[§] Ian J. Clifton, Peter L. Roach,[||] Jack E. Baldwin, Peter J. Rutledge,[⊥] and Christopher J. Schofield*

Chemistry Research Laboratory, University of Oxford, Mansfield Road, Oxford OX1 3TA, U.K.

Received December 1, 2004; Revised Manuscript Received March 7, 2005

ABSTRACT: Isopenicillin N synthase (IPNS), a non-heme iron(II)-dependent oxidase, catalyzes conversion of the tripeptide δ-(L-α-aminoadipoyl)-L-cysteinyl-D-valine (ACV) to bicyclic isopenicillin N (IPN), concomitant with the reduction of dioxygen to two molecules of water. Incubation of the "truncated" substrate analogues δ-(L-α-aminoadipoyl)-L-cysteinyl-glycine (ACG) and δ-(L-α-aminoadipoyl)-L-cysteinyl-D-alanine (ACA) with IPNS has previously been shown to afford acyclic products, in which the substrate cysteinyl residue has undergone a two-electron oxidation. We report X-ray crystal structures for the anaerobic IPNS/Fe(II)/ACG and IPNS/Fe(II)/ACA complexes, both in the absence and presence of the dioxygen analogue nitric oxide. The overall protein structures are very similar to those of the corresponding IPNS/Fe(II)/ACV complexes; however, significant differences are apparent in the vicinity of the active site iron. The structure of the IPNS/Fe(II)/ACG complex reveals that the C-terminal carboxylate of this substrate is oriented toward the active site iron atom, apparently hydrogen-bonded to an additional water ligand at the metal; this is a different binding mode to that observed in the IPNS/Fe(II)/ACV complex. ACA binds to the metal in a manner that is intermediate between those observed for ACV and ACG. The addition of NO to these complexes initiates conformational changes such that both the IPNS/Fe(II)/ACG/NO and IPNS/Fe(II)/ACA/NO structures closely resemble the IPNS/Fe(II)/ACV/NO complex. These results further demonstrate the feasibility of metal-centered rearrangements in catalysis by non-heme iron enzymes and provide insight into the delicate balance between hydrophilic−hydrophobic interactions and steric effects in the IPNS active site.

The biosynthesis of the medicinally important penicillin family of antibiotics involves an unusual oxidative bicyclization reaction catalyzed by isopenicillin N synthase (IPNS)[1], a non-heme ferrous iron-dependent oxidase that is structurally related to the 2-oxoglutarate-dependent family of oxygenases. The desaturative bicyclization of δ-(L-α-aminoadipoyl)-L-cysteinyl-D-valine (ACV, **1**) to isopenicillin N (IPN, **2**) is coupled to the reduction of dioxygen to water (Figure 1a) (*1*). Extensive studies on IPNS have led to the proposal of a mechanism in which closure of the β-lactam ring precedes formation of the thiazolidine ring and in which the second cyclization is mediated by a reactive iron(IV)−oxo intermediate (Fe(IV)═O ↔ Fe(III)−O•) (*2*−*5*).

Incubation of highly purified recombinant IPNS with an array of substrate analogues has been used to test the selectivity of the enzyme (*3*); structural analysis of the resulting products has demonstrated that IPNS can carry out various different types of oxidative reaction. The results obtained with the "truncated" substrate analogues δ-(L-α-aminoadipoyl)-L-cysteinyl-glycine (ACG, **3**) and δ-(L-α-aminoadipoyl)-L-cysteinyl-D-alanine (ACA, **4**) (formed by replacement of the D-valine residue by glycine and D-alanine, respectively) are interesting, since neither of these analogues gives rise to cyclic products upon incubation with IPNS (Figure 1b,c). Thus, when ACG was incubated with IPNS,

[†] This work was supported by the Wellcome Trust, the BBSRC, and EPSRC, U.K. and the E.U. A.J.L. was supported by the BBSRC, P.L.R. by the Royal Society, and P.J.R. by the Rhodes Trust.

[‡] Atomic coordinates and structure factors have been deposited in the Protein Databank, Research Collaboratory for Structural Bioinformatics, Rutgers University, New Brunswick, NJ (http://www.rcsb.org/). Accession codes: 1w03 for IPNS/Fe(II)/ACG, 1w04 for IPNS/Fe(II)/ACG/NO, 1w05 for IPNS/Fe(II)/ACA, and 1w06 for IPNS/Fe(II)/ACA/NO.

* To whom correspondence should be addressed: Chemistry Research Laboratory, University of Oxford, Mansfield Road, Oxford OX1 3TA, U.K. Phone, +44 1865 275625; fax, +44 1865 275674; e-mail, christopher.schofield@chem.ox.ac.uk.

[§] Current address: AstraZeneca Avlon Works, Severn Road, Bristol, BS10 7ZE, U.K.

[||] Current address: Department of Chemistry, University of Southampton, Highfield, Southampton, SO17 1BJ, U.K.

[⊥] Current address: Centre for Synthesis & Chemical Biology, Department of Chemistry, University College Dublin, Belfield, Dublin 4, Ireland.

[1] Abbreviations: ACV, δ-(L-α-aminoadipoyl)-L-cysteinyl-D-valine; ACG, δ-(L-α-aminoadipoyl)-L-cysteinyl-glycine; ACA, δ-(L-α-aminoadipoyl)-L-cysteinyl-D-alanine; CCD, charge couple device; CCP4, Collaborative Computational Project Number 4; EDCI, 1-(3-dimethylaminopropyl)-3-ethylcarbodiimidehydrochloride; ESRF, European Synchrotron Research Facility; HOBt, 1-hydroxybenzotriazole hydrate; HPLC, high-performance liquid chromatography; ID, insertion device; IPN, isopenicillin N; IPNS, isopenicillin N synthase; ODS, octadecylsilane; rms, root mean square; SRS, Synchrotron Radiation Source; Wat, water molecule.

10.1021/bi047478q CCC: $30.25
Published on Web 04/08/2005

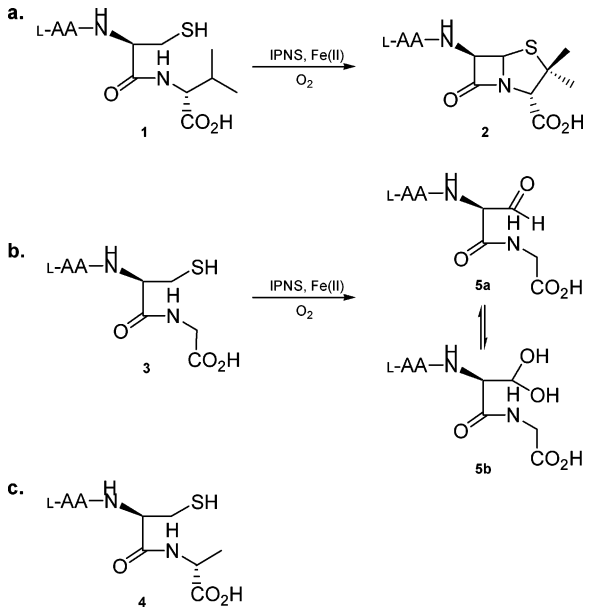

FIGURE 1: (a) The overall reaction of IPNS with ACV **1**; (b) the reaction of ACG **3** with IPNS; (c) the structure of ACA **4**; L-AA = L-δ-(α-aminoadipoyl).

the resultant incubation mixture gave no indication of β-lactam-derived signals in the ^{1}H NMR but led to the observation of a characteristic resonance at 89 ppm in the ^{13}C NMR spectrum of the product (*6*). Comparison with an authentic synthetic sample showed that the predominant product isolated from this incubation was the hydrated aldehyde **5a,b** (*6*), which results from a two-electron oxidation of the tripeptide substrate (in contrast to the four-electron oxidation required for penicillin formation). This uncoupling of oxidation at the cysteinyl β-position from the thiazolidine ring closure in IPNS catalysis reflects the close relationship between the mechanisms of IPNS and the 2-oxoglutarate-dependent oxygenases. In the latter systems, uncoupling of 2-oxoglutarate oxidation from oxidation of the primary substrate has been observed in a number of cases, brought about either by mutagenesis or through the use of substrate analogues (*7*−*10*). Several mechanisms can be envisaged to explain formation of the hydrated aldehyde from ACG. One involves a reaction to form the thioaldehyde intermediate **6**, which is hydrolyzed to the aldehyde without closure of a β-lactam ring (Figure 2, path a). Alternatively, a monocyclic β-lactam intermediate **7** may form (as proposed in the conversion of ACV to IPN), which can then collapse to give the acyliminium ion **8**. This intermediate could be trapped by water to give the alcohol **9**, which will rapidly ring open (Figure 2, path b). Incubation experiments with labeled ACG analogues and sodium borotritiide have not furnished conclusive evidence in favor of one pathway or the other (*11*), and the process by which the catalytic cycle is completed and, in particular, how the active site metal is returned to the iron(II) oxidation state remain unclear.

Unlike ACG **3**, the ACA analogue **4** can, in theory, form a bicyclic β-lactam product by thiazolidine closure onto the β-carbon of alanine. However, when ACA was incubated with IPNS in a previous study, no evidence for β-lactam formation was obtained by ^{1}H NMR analysis and no antibiotic product was discernible by hole−plate bioassay (*12*). These incubation experiments were repeated as part of the current study, ACA being incubated with IPNS following the previously reported procedure (*13*) and the incubation mixture analyzed by hole−plate bioassay (*14*). Incubation and bioassay of ACV was used as a positive control, and kill zones (indicative of penicillin products) were clearly visible around holes containing the ACV-derived incubation mixture. There was no evidence of antibiotic activity around holes containing the incubation mixture of ACA, and ^{1}H NMR analysis of this reaction mixture showed no evidence

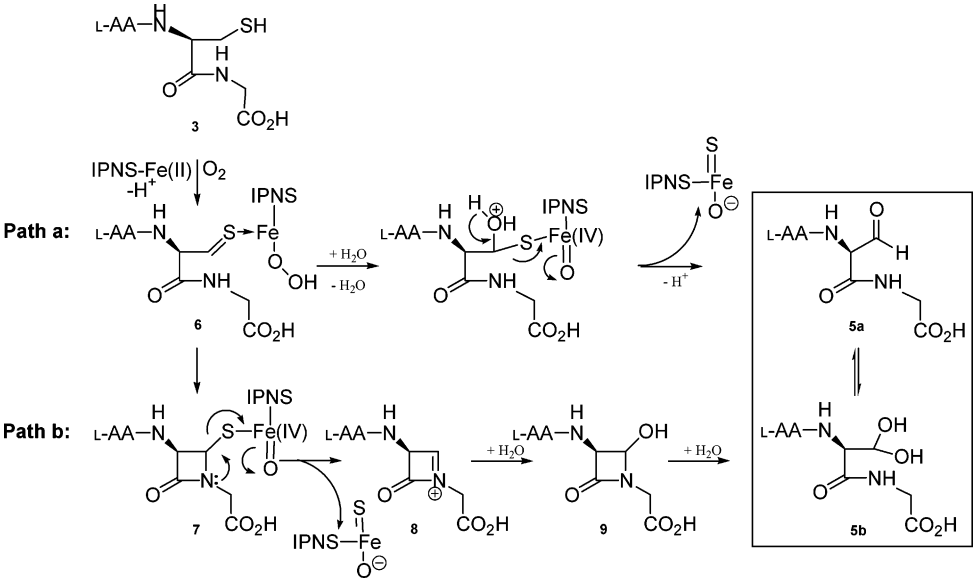

FIGURE 2: Possible mechanisms for the reaction of IPNS with ACG. Note that the conversion of ACG **3** to the aldehyde **5** requires a two-electron oxidation; in contrast to the conversion of ACV to IPN, only half the oxidizing power of dioxygen is used. This is interesting because IPNS is closely related to the 2-oxoglutarate (2-OG)-dependent iron(II) oxygenases; in catalysis by these enzymes, both 2-OG and the primary substrate undergo two-electron oxidation. Thus, the two-electron oxidation of ACG by IPNS provides a mechanistic link with the 2-OG-dependent enzymes. In the IPNS-catalyzed turnover of ACG, there must be a way by which the iron(IV) form of the enzyme is reduced to the iron(II) form required for initiation of a subsequent catalytic cycle. This may occur via the extrusion of atomic sulfur (*6*), although there is no direct evidence for this. Alternatively, the iron(IV) species could be reduced by reaction with a thiol such as dithiothreitol (present in the incubation mixture) or another molecule of the substrate (itself a thiol). L-AA = L-δ-(α-aminoadipoyl).

for β-lactam products. These experiments confirm the results reported previously, that ACA is not converted to penicillin products by IPNS, but it was not possible to determine if a hydrated aldehyde product (equivalent to the "δ_{89}" compound **5a,b** formed from incubation of ACG with IPNS) is formed instead.

It has been proposed that thiazolidine ring closure in the formation of IPN involves C−H abstraction from the valinyl β-center to give a tertiary carbon-centered radical (*15*). By analogy, formation of a penam product from ACA would require a less favorable C−H abstraction from the methyl carbon to form an unstable primary radical. However, the relative instability of primary versus tertiary radicals cannot, on its own, explain the lack of bicyclic product formation from ACA; when δ-(L-α-aminoadipoyl)-L-cysteinyl-D-α-aminobutyrate (ACAb) was incubated with IPNS, one of the products formed was a cepham (*16*), demonstrating that IPNS can mediate ring closure between the cysteinyl sulfur and a methyl group.

The solution of crystal structures for IPNS in complex with manganese(II) (*17*) and IPNS complexed with iron(II) and its substrate ACV (*4*) has allowed a new approach to the study of IPNS catalysis. Herein, we describe the application of protein crystallography to investigate the reactions of IPNS with the truncated substrate analogues ACG and ACA.

MATERIALS AND METHODS

Synthesis of Substrate Analogues. N-tert-Butyloxycarbonyl-α-*p*-methoxybenzyl-δ-L-aminoadipic acid and *S*-benzhydryl-L-cysteine were prepared from the free amino acids and coupled using the reported procedure for activation with *iso*-butyl chloroformate (*18*, *19*). Fully protected ACG was obtained by coupling the protected aminoadipoyl−cysteine dipeptide to glycine *tert*-butyl ester (Aldrich), using 1-(3-dimethylaminopropyl)-3-ethylcarbodiimidehydrochloride (EDCI) and 1-hydroxybenzotriazole hydrate (HOBt) (*20*). Similarly, fully protected ACA was obtained by coupling the aminoadipoyl−cysteine dipeptide to D-alanine benzhydryl ester (prepared from D-alanine by reaction with *p*-toluenesulfonic acid and diphenyldiazomethane (*21*)). Trifluoroacetic acid-mediated deprotection (*19*) and HPLC purification afforded each of the tripeptides in pure form for crystallization with IPNS. HPLC conditions: ODS (250 mm × 10 mm), 10 mM NH_4HCO_3 in water/methanol as eluant (0−6 min, 2.5%; 6−14 min, 25%; 14−20 min, 2.5% methanol v/v), 4 mL/min, λ = 254 nm, 5 AUFS; R_t (ACG), 4.5 min; R_t (ACA), 4.2 min.

Crystallization and NO Exposure. Crystals of IPNS/Fe(II)/ACG and IPNS/Fe(II)/ACA (ca. 0.6 mm × 0.2 mm × 0.1 mm) were grown under anaerobic conditions (*22*). Three morphologies of IPNS crystals have previously been reported to grow under these conditions: an orthorhombic plate form of space group $P2_12_12_1$, a hexagonal form of space group $P3_12_1$, and a needle form which does not diffract sufficiently to allow space group determination. Crystals of all three morphologies were observed from the crystallization of IPNS with both ACG and ACA, and data were collected from crystals of both plate and hexagonal forms.

Crystals to be used for the determination of the IPNS/Fe(II)/ACG and IPNS/Fe(II)/ACA structures were removed from the anaerobic environment, exchanged into cryoprotectant buffer (*22*), and flash-frozen in liquid nitrogen. For the preparation of NO complexes, crystals were exposed to nitric oxide as previously described (*4*) then removed from the glovebox and flash-frozen.

Data Collection. Data were collected at 100 K using either the Cu Kα radiation from a Rigaku rotating anode generator operating at 60 kV and 70 mA and a 300 mm MAR Research image plate detector at the Department of Molecular Biophysics, Oxford, U.K. (IPNS/Fe(II)/ACG and IPNS/Fe(II)/ACA complexes), the synchrotron radiation at beamline 9.6 at the Synchrotron Radiation Source (SRS), Daresbury, U.K. and a 300 mm MAR Research Plate image plate detector (IPNS/Fe(II)/ACG/NO complex), or the synchrotron radiation at beamline BM14 of the European Synchrotron Research Facility (ESRF), Grenoble, France, equipped with a 300 mm MAR Research Plate image plate detector (IPNS/Fe(II)/ACA/NO) (Table 1).

Structure Determination. Data were indexed and integrated with Denzo (*23*) or Mosflm (*24*) and scaled using Scalepack (*23*) or Scala from the CCP4 suite of programs (*25*). Initial structures were generated by rigid body refinement of protein atoms from the IPNS/Fe(II)/ACV model (*4*) against the new data. Further refinement was carried out with prolsq (*25*), Xplor (*26*), SHELXL (*27*) and REFMAC (*25*). The final round of refinement for all structures was performed with REFMAC. Electron density maps were interpreted using the program O (*28*). The active site iron atom and water molecules were added in the course of refinement. There was clear electron density visible for substrate-derived species throughout refinement; however, substrate atoms were only included in refinement once their position could be assigned unambiguously from electron density. Iron−ligand bond lengths were unrestrained throughout refinement. Note that it is not certain that NO ligates to iron via its nitrogen atom.

Color figures were prepared using the programs MolScript (*29*), BobScript (*30*) and Raster3D (*31*).

RESULTS

Structure of the Anaerobic IPNS/Fe(II)/ACG Complex. The structure of the IPNS/Fe(II)/ACG complex was solved to 2.10 Å resolution from a crystal of plate morphology (Figure 3a). The overall structure of the protein is very similar to the IPNS/Fe(II)/ACV structure (*4*) (rms difference between C_α chains, 0.13). As in the IPNS/Fe(II)/ACV complex, the substrate lies in an extended conformation with the L-α-aminoadipoyl carboxylate anchored by a salt bridge to Arg 87. The iron atom is ligated by the side chains of three residues, His 214, Asp 216, and His 270 (making up the triad motif that is highly conserved across the family of non-heme iron enzymes to which IPNS belongs (*7*, *32*)), a water molecule in the site opposite His 214 (Wat_A, to simplify comparison between structures, key active site water molecules are represented using this notation, an explanation of which is given in Figure 4 and Table 2), and the cysteinyl thiolate of the tripeptide substrate. However, ACG binds differently to ACV in the region of its C-terminal amino acid.

When ACV binds at the IPNS active site, a water ligand is displaced from the site trans to Asp 216 and its place is taken by the valinyl isopropyl group of the substrate, which

Table 1: Data Collection and Statistics

complex	IPNS/Fe(II)/ACG		IPNS/Fe(II)/ACG/NO		IPNS/Fe(II)/ACA		IPNS/Fe(II)/ACA/NO	
PDB accession code	1w03		1w04		1w05		1w06	
X-ray source	rotating anode		beamline 9.6, SRS		rotating anode		BM14, ESRF	
Wavelength λ (Å)	1.5418		0.8700		1.5418		0.9970	
Space group	$P2_12_12_1$		$P2_12_12_1$		$P3_121$		$P2_12_12_1$	
Unit cell (a (Å), b (Å), c (Å))	46.77, 71.20, 100.97		46.65, 70.75, 100.97		101.77, 101.77, 115.68		47.13, 71.45, 101.88	
resolution shell (Å)	30.00−2.10	2.18−2.10	16.10−1.28	1.35−1.28	25.40−2.46	2.54−2.46	28.63−1.65	1.74−1.65
measurements	143182	5868	290686	33873	76481	7081	99143	14092
average $I/\sigma I$	5.1	3.6	10.8	3.2	12.42	2.17	10.0	2.2
unique reflections	20279	1761	79891	10613	24819	2310	37540	5242
completeness (%)	98.2	87.3	92.6	85.3	96.5	98.8	88.5	85.6
R_{merge} (%)[a]	13.1	37.8	7.8	32.5	11.9	58.1	10.5	40.5
R_{cryst} (%)[b]	17.2		16.3		16.2		17.1	
R_{free} (%)[c]	19.7		17.5		21.4		20.4	
rms deviation[d]	0.019 Å (1.9°)		0.023 Å (2.0°)		0.030 Å (2.2°)		0.018 Å (1.7°)	
B factors[e] (Å^2)	17.8, 18.9, 7.6, 36.2		6.6, 8.5, 8.0, 22.3		25.7, 27.9, 38.2, 44.2		9.6, 12.2, 11.8, 30.7	
residues	329		329		329		329	
water molecules	327		272		317		339	

[a] $R_{merge} = (\sum_j\sum_h$×e7$I_{h,j}$-$\langle I_h\rangle$×e7/$\sum_j\sum_h\langle I_h\rangle) \times 100$. [b] $R_{cryst} = (\sum$×e7×e7F_{obs}×e7− ×e7F_{calc}×e7×e7/$\sum$×e7F_{obs}×e7) × 100. [c] R_{free} is based on 5% of the total reflections. [d] The rms deviation from ideality for bonds (followed by the value for angles). [e] Average B factors in order: main chain, side chain, substrate, and solvent.

sits within van der Waals contact distance of the iron. Thus, in the IPNS/Fe(II)/ACV complex, the iron is pentacoordinate and its coordination geometry square pyramidal (*4*). In contrast, the iron atom in the IPNS/Fe(II)/ACG complex remains hexacoordinate even with ACG bound: the fifth and sixth coordination sites are occupied by water molecules (Wat_A and Wat_F). Furthermore, the glycinyl portion of the tripeptide assumes a markedly different conformation to that taken up by the ACV valine. In the ACV complex, the cysteinyl−valine peptide bond of the substrate sits roughly parallel to the C_α−C_β bond of cysteine, the cysteinyl carbonyl group points away from iron, and the valinyl N−H is oriented toward the metal (*4*). Thus, the cysteinyl CO, C_α, and C_β and the valinyl NH are approximately coplanar, approaching the conformation required for β-lactam formation; the valinyl carboxylate is oriented away from iron and held by a network of hydrogen bonds to the side chains of Tyr 189, Ser 281, and Arg 279. In contrast, the glycinyl carboxylate of ACG points toward iron and appears to be tethered via hydrogen bonding to Wat_F; the glycinyl carboxylate also maintains a link to Arg 279 via hydrogen bonds between its other oxygen atom and Wat_B. The C_α−CO bond of ACG cysteine is rotated by ca. 33° (relative to the equivalent bond in the IPNS/Fe(II)/ACV complex) such that its carbonyl oxygen is directed more toward iron and the glycinyl N−H angled away (and, as a result, the two hydrogen atoms that must be removed to effect β-lactam formation are no longer close to each other or the putative oxygen binding site). The side chain of Arg 279 is twisted slightly relative to the IPNS/Fe(II)/ACV structure, presumably so that it can maintain a bidentate hydrogen bonding arrangement with Wat_B.

Overall the IPNS/Fe(II)/ACG complex incorporates three more water molecules in the immediate vicinity of iron relative to the IPNS/Fe(II)/ACV structure: Wat_F which occupies the site trans to Asp 216 and two others (Wat_G and Wat_H) approximately filling the space that would normally be taken up by the valinyl side chain. Furthermore, the conformational changes that have occurred appear to exclude the water molecule that is observed between the substrate and Phe 211 in the IPNS/Fe(II)/ACV structure (Wat662 in the PDB submission 1bk0).

Structure of the IPNS/Fe(II)/ACG/NO Complex. The structure of the IPNS/Fe(II)/ACG/NO complex was solved to 1.28 Å resolution (Figure 3b). The introduction of NO induces a significant change in the conformation of ACG at the IPNS active site. Whereas the IPNS/Fe(II)/ACG structure differed significantly from the IPNS/Fe(II)/ACV complex in the region of the iron, the IPNS/Fe(II)/ACG/NO and the IPNS/Fe(II)/ACV/NO structures are very similar: the iron is hexacoordinate in both complexes, NO is bound in the site trans to Asp 216 in both, and the two structures are very alike with respect to overall number and position of atoms in the active site. In the one significant difference between the structures, the space occupied by the valinyl isopropyl group in the ACV complex is filled in the IPNS/Fe(II)/ACG/NO complex by a single water molecule (Wat_I) hydrogen-bonded to Wat_A. (The position of this new water molecule Wat_I is different to those of both Wat_G and Wat_H seen in the anaerobic IPNS/Fe(II)/ACG complex.)

Structure of the IPNS/Fe(II)/ACA Complex. The structure of the IPNS/Fe(II)/ACA complex was solved to 2.46 Å resolution (Figure 3c) from a crystal of hexagonal morphology. As observed in the IPNS/Fe(II)/ACG complex, the protein backbone remains virtually unchanged in the presence of the modified substrate (the rms difference is 0.23 for C_α chains of the ACV and ACA complexes, 0.19 for the C_α chains of the ACG and ACA complexes).

The L-α-aminoadipoyl tail of ACA is bound in the same extended conformation as that of the ACV complex. However, at the other terminus of the tripeptide, the plane of the

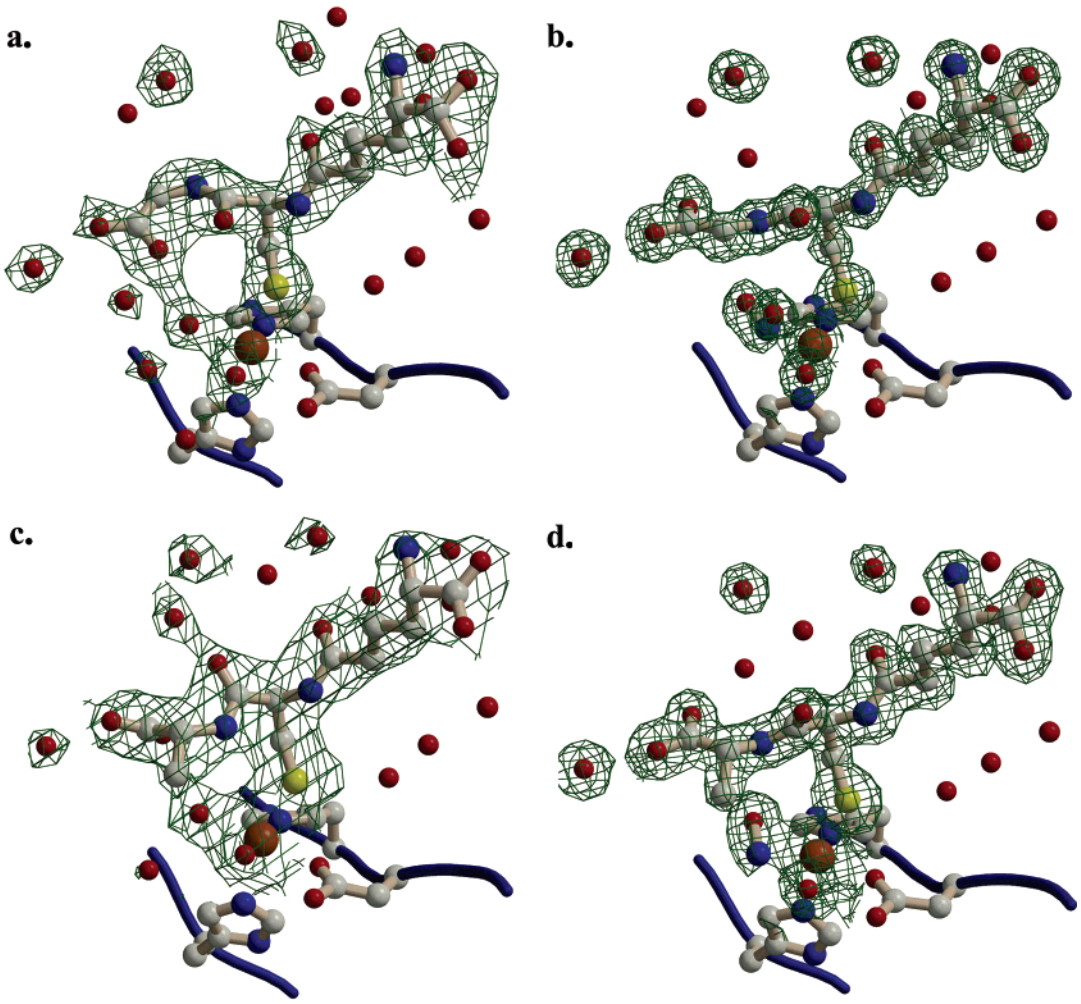

FIGURE 3: The active site region of the IPNS/Fe(II)/substrate complexes. (a) The anaerobic IPNS/Fe(II)/ACG complex (1w03); (b) the IPNS/Fe(II)/ACG/NO complex (1w04); (c) the anaerobic IPNS/Fe(II)/ACA complex (1w05); and (d) the IPNS/Fe(II)/ACA/NO complex (1w06). Relevant sections of the protein backbone are shown (blue ribbon), and for clarity only, the three iron-binding side chains (His 214, Asp 216, and His 270) are drawn. Electron density maps ($2mF_{obs} - DF_{calc}$ maps contoured at 1σ) are shown only for tripeptide substrates, iron (orange), NO, and key water molecules.

alanyl carboxylate is tilted "backwards" ca. 38° relative to the valinyl carboxylate of ACV. As in the ACG complex (Figure 3a), the binding of ACA does not displace the coordinated water ligand opposite Asp 216 (Wat_F), and the iron is hexacoordinate. There is also a second extra water molecule (Wat_H) in the active site region compared to the ACV complex, occupying the space that would otherwise be filled by one of the methyl groups of ACV valine. The plane of the cysteinyl−alanine peptide bond is tilted "backwards" through ca. 86° relative to the equivalent bond in ACV. Thus, as in the IPNS/Fe(II)/ACG structure, the N−H atom of the cysteinyl−alanine amide bond does not point toward the putative oxygen binding site, and the four atoms that might form a β-lactam ring are not coplanar. Finally, the oxygen atom of the cysteinyl carbonyl group appears to hydrogen-bond to a water molecule "behind" the substrate (Z195), in contrast to the arrangement observed in the IPNS/Fe(II)/ACV complex.

Structure of the IPNS/Fe(II)/ACA/NO Complex. The structure of the IPNS/Fe(II)/ACA/NO complex was solved to 1.65 Å resolution (Figure 3d). As seen in the ACG case, the conformation of the substrate changes upon the introduction of NO such that the active site region of the IPNS/Fe(II)/ACA/NO complex closely mirrors the IPNS/Fe(II)/ACV/NO complex. Nitric oxide displaces the water ligand trans to Asp 216 (Wat_F), and NO binding also results in extrusion of the second additional water molecule (Wat_H) from the space left vacant by the valinyl isopropyl group in the IPNS/Fe(II)/ACA complex. As was seen with ACG, upon NO binding, the four atoms that would hypothetically form a β-lactam move into a plane, and the cysteinyl *pro*-3*S* hydrogen and the alanyl NH both point toward the oxygen mimic. The cysteinyl carbonyl also moves into a position from which it could hydrogen-bond to a water molecule (Z326, Wat_C) "above" the substrate, as seen for ACV.

DISCUSSION

The IPNS Complexes with ACG. In the complex of IPNS with its natural substrate ACV, the valinyl carboxylate is oriented away from iron, interacting with hydrophilic residues in a water-filled region of the active site; the isopropyl group of the substrate sits in close proximity to the metal, filling the iron binding site trans to Asp 216 (Figure 4a) (*4*). In this way, the size and hydrophobic nature of the valine side chain apparently prevent water from entering the sixth binding site at iron and thereby prime the enzyme for reaction with dioxygen. (A similar situation is seen for the 2-oxoglutarate-dependent oxygenases, homologously related to

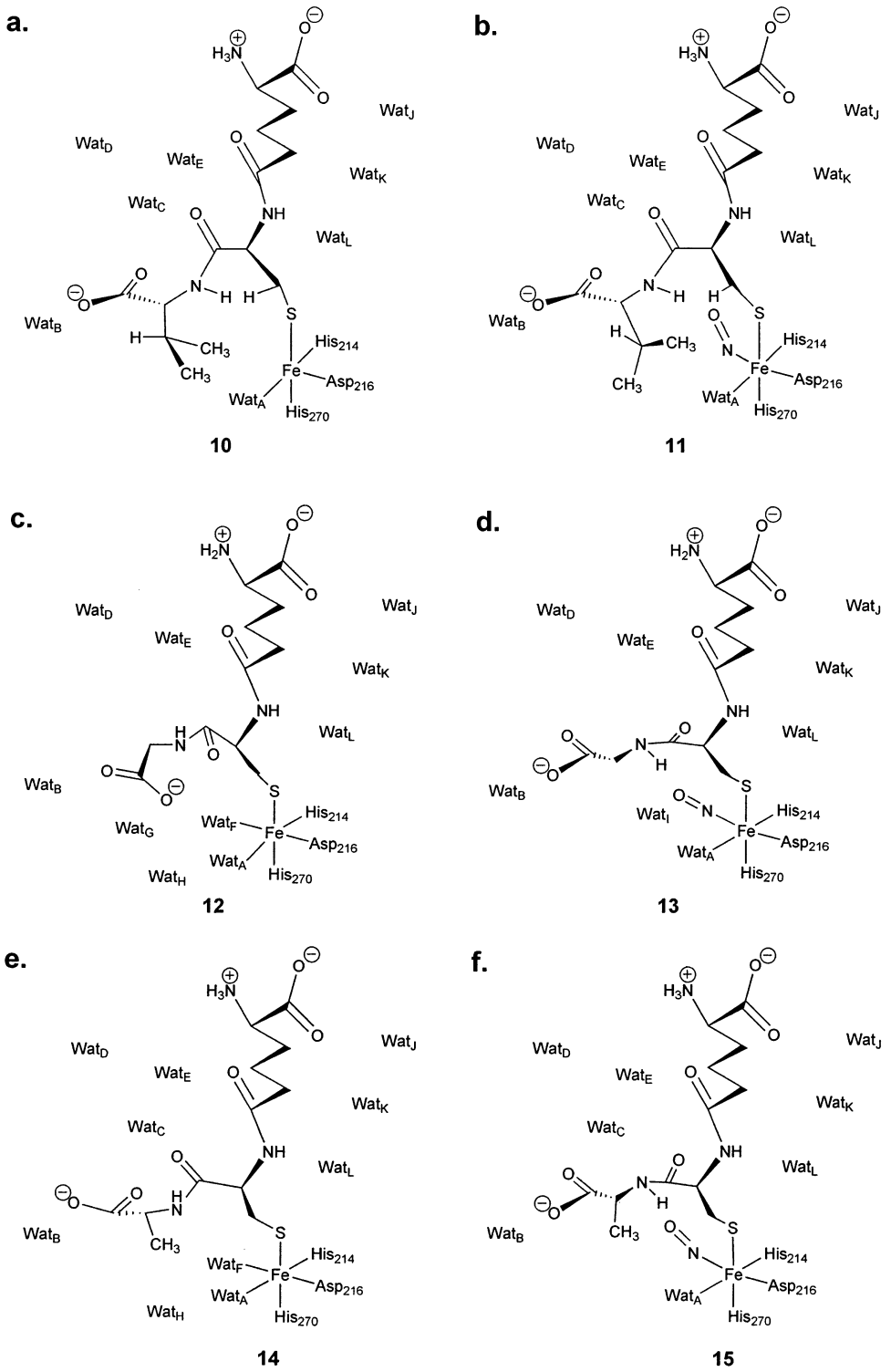

FIGURE 4: Stylized representations to show key water molecules in the active site region. The IPNS active site with (a) ACV, (b) ACV + NO, (c) ACG, (d) ACG + NO, (e) ACA, and (f) ACA + NO bound to iron. Note that this representation does not aim to comprehensively represent every water molecule in the region, rather to highlight and define the key crystallographic waters that are discussed in the text. This figure works in conjunction with Table 2 to highlight these key water molecules and provide a link with the structures deposited in the PDB.

IPNS, in which binding of the "primary" substrate is proposed to activate iron in a comparable fashion (*33*−*35*).) The glycine residue in ACG is much less hydrophobic than valine in the natural substrate and offers less steric hindrance to the entry of water. It appears that these two factors permit a conformational change in substrate binding relative to the IPNS/Fe(II)/ACV structure: in the IPNS/Fe(II)/ACG complex (Figures 3a and 4c), there is an additional water ligand at iron (Wat_F in the binding site opposite Asp 216) and the glycinyl carboxylate is oriented toward the metal, interacting with the iron-bound Wat_F (while also maintaining a link with Arg 279). It is difficult to see how ACV could occupy an analogous conformation because of its greater side chain bulk and because doing so would place the hydrophobic isopropyl

Table 2: Correlation of Key Water Molecules Discussed in Text with Structures in PDB

	structure					
water	ACV (1bk0)	ACVNO (1blz)	ACG (1w03)	ACGNO (1w04)	ACA (1w05)	ACANO (1w06)
A	Wat713	Wat650	Z188	Z230	Z226	Z333
B	Wat714	Wat523	Z268	Z240	Z315	Z332
C	Wat692	Wat738			Z310	Z326
D	Wat629	Wat673	Z65	Z37	Z312	Z325
E	Wat590	Wat712	Z264	Z316	Z317	Z327
F			Z267		Z311	
G			Z235			
H			Z1		Z105	
I				Z314		
J	Wat709	Wat532	Z269	Z319	Z316	Z331
K	Wat704	Wat531	Z190	Z232	Z228	Z240
L	Wat710	Wat514	Z189	Z231	Z227	Z239

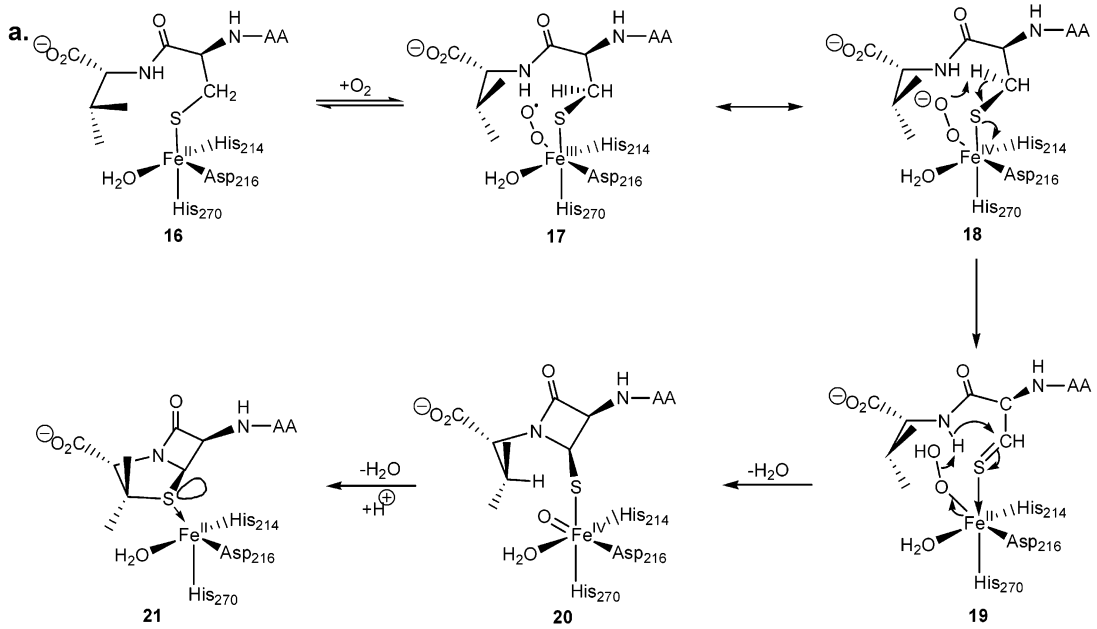

FIGURE 5: Proposed mechanism for the reaction of IPNS with ACV (*4*).

group into a hydrophilic region of the active site (close to the polar side chains of residues Thr 331 and Tyr 189).

When NO is introduced to the ACV complex, it displaces the valinyl isopropyl group and binds to iron opposite the carboxylate ligand Asp 216 (*4*). In so doing, NO does not significantly alter the hydrophobicity of this region. In the IPNS/Fe(II)/ACV/NO complex (Figure 4b), the number of water molecules in the active site region is unchanged by NO binding and the conformation of the substrate changes only slightly (the isopropyl side chain rotates ca. 33° to make room for NO). In contrast, when NO binds to the IPNS/Fe(II)/ACG complex, the water molecule that was bound trans to Asp 216 (Wat_F) is displaced, disrupting the link between the glycinyl carboxylate and iron and changing the overall hydrophobicity of the active site (Figures 3b and 4d). The substrate reorients to interact with Arg 279 in the same manner as ACV, an arrangement that now appears to be the most thermodynamically favorable option available to the system. This change increases the hydrophobicity of the area close to the iron, which forces two other water molecules (Wat_G and Wat_H) out of the active site region. There is still one additional water molecule (Wat_I) in the active site region of the IPNS/Fe(II)/ACG/NO structure relative to the IPNS/Fe(II)/ACV/NO complex, presumably allowed in by the smaller size of the glycinyl side chain. Crystallographic studies with the related dioxygenase clavaminic acid synthase (CAS) have shown rearrangement of the 2-oxoglutarate cosubstrate upon NO binding (*36*), and it is possible that metal-centered rearrangements are a common feature of catalysis by members of this enzyme family.

The mechanism previously proposed for β-lactam formation from ACV involves reduction of dioxygen to superoxide by electron transfer from iron (Figure 5) (*4*). It is thought that the resulting superoxide species **17**/**18** removes the *pro*-3*S* hydrogen from the ACV cysteine to give a thioaldehyde, producing the hydroperoxide intermediate **19** in which iron has been reduced back to the ferrous state. Cleavage of the O−O bond with concomitant removal of the valinyl N−H proton and attack by nitrogen on the thioaldehyde would effect β-lactam closure and give rise to the ferryl intermediate **20**. The high-valent iron species in **20** is proposed to mediate thiazolidine closure in a subsequent step. Direct evidence for a ferryl intermediate has previously been reported for another enzyme from the 2-oxoglutarate oxygenase family, taurine/alpha-ketoglutarate dioxygenase (TauD) (*37*−*39*).

The structure of the unexposed IPNS/Fe(II)/ACG complex shows the cysteinyl−glycine amide NH to be oriented away from iron, and so away from any putative metal-bound

reactive oxygen species. This would militate against the reaction to form a β-lactam intermediate from ACG (akin to the fourth step in Figure 5, **19** → **20**, in which the amide nitrogen attacks the thioaldehyde and is deprotonated). Considered in isolation, therefore, this structure suggests that ACG oxidation to the hydrated aldehyde **5** does not proceed via a monocyclic β-lactam intermediate (ruling out path a, Figure 2). However, the introduction of NO changes this interpretation significantly. After NO binding, the glycinyl nitrogen lies almost in the same plane as the cysteinyl CO, C_α, and C_β, a similar arrangement to that seen in both the IPNS/Fe(II)/ACV and IPNS/Fe(II)/ACV/NO complexes. In this orientation, the *pro*-3*S* hydrogen of cysteine and the glycinyl NH are both in positions from which they could conceivably react with iron−oxygen species to generate a monocyclic β-lactam intermediate. Thus the IPNS/Fe(II)/ACG structures do not indicate conclusively whether the δ_{89} analogue **5** is formed via a β-lactam intermediate (Figure 2, path a) or not (Figure 2, path b), but they do suggest it is possible on structural grounds.

The IPNS/Fe(II)/ACA Complexes. ACA also has a smaller, less hydrophobic side chain than ACV does, and this allows two extra water molecules into the active site of the anaerobic IPNS/Fe(II)/ACA complex, including an additional water ligand at iron, Wat_F (Figures 3c and 4e). The presence of ACA in the active site also facilitates an altered substrate conformation relative to the IPNS/Fe(II)/ACV case (Figure 4a), presumably in order to maximize hydrogen bonding interactions. However, the side chain of alanine is more hydrophobic than that of the glycine, so it is more favorable for the alanyl side chain to bind in the hydrophobic pocket normally occupied by the valinyl isopropyl group than anywhere else. Thus, the C-terminal carboxylate of the ACA tripeptide binds to Arg 279 similarly, although not identically, to the ACV carboxylate, rather than twisting around further to hydrogen-bond to the water ligand at iron (Wat_F) as in the ACG complex. If ACA was to bind in a conformation akin to ACG, the alanyl side chain would be forced into the hydrophilic and more sterically restricted environment near to Wat_C "above" the substrate.

The introduction of NO to the IPNS/Fe(II)/ACA complex alters the active site region, apparently making it more hydrophobic and extruding the two "extra" water molecules present in the IPNS/Fe(II)/ACA complex. The IPNS/Fe(II)/ACA/NO structure (Figures 3d and 4f) shows both the cysteinyl *pro*-3*S* and alanyl NH hydrogens in positions from which they would be able to react with iron-bound oxygen species, which would allow a mechanism akin to that proposed for reaction of the natural substrate ACV. Furthermore, the alanyl β-carbon is in essentially the same position as that occupied by C_β of valine in the IPNS/Fe(II)/ACV/NO complex. Assuming that reaction intermediates arising from ACA and ACV would also have similar conformations, the alanyl β-hydrogen atoms of ACA would sit in approximately the same position relative to the ferryl oxygen in an ACA-derived monocyclic intermediate equivalent to **20**. This suggests that the failure of IPNS to convert ACA into penicillin products is not principally due to differences in the relative conformations of the two peptides at the active site (despite the important differences that are evident between the IPNS/Fe(II)/ACV and IPNS/Fe(II)/ACA structures) and that other factors must also be involved.

Conclusions. The results described above demonstrate that reducing the size and hydrophobicity of the valinyl side chain of ACV allows additional water molecules into the active site region of IPNS, even after dioxygen binding (assuming that the binding of NO to the anaerobic IPNS/Fe(II)/substrate complexes provides an accurate reflection of dioxygen binding). This, in itself, may explain the observed outcome of the IPNS reaction with ACG and ACA: the failure of either to afford β-lactam products may arise directly from the interception of reactive intermediates by the additional water molecules in the active site. However, two-electron oxidation products have been isolated from the reaction of ACG with IPNS (*6*), indicating that oxidation at the cysteinyl β-carbon can still occur. It is possible that the decreased hydrophobicity of the alanyl and glycinyl side chains (relative to valine) might allow alternative hydrogen bonding interactions between hydroperoxide and thioaldehyde moieties in reaction intermediates akin to **19** (Figure 5), preventing further oxidation and blocking β-lactam formation. Release of a thioaldehyde from the enzyme is unlikely (*40*, *41*), but attack on such an intermediate by a water molecule (with the active site iron acting as a Lewis acid catalyst, a role it has been observed to play in other contexts (*42*)) could lead to the aldehyde product observed in the case of ACG and a related product (as yet undetected) from the reaction of ACA. Alternatively, if a monocyclic β-lactam intermediate was to be formed from either of these analogues, it could be that an additional active site water molecule facilitates collapse to the acyl-iminium ion, or even promotes direct reduction of the ferryl intermediate by an extraneous reducing agent (or that the more hydrophilic, less constrained nature of the active site slows or precludes thiazolidine ring closure in the ACA case).

In considering the effects of hydrophobicity on the catalytic activity of IPNS, we note that ACV analogues in which valine is replaced by residues bearing polar side chains are generally poor substrates for the enzyme. Few such analogues have been converted to bicyclic products by IPNS (*3*). In contrast a wide range of analogues bearing purely hydrocarbon (i.e., hydrophobic) side chains are turned over by IPNS, giving a variety of bicyclic penam and cepham products (*3*). For example, δ-(L-α-aminoadipoyl)-L-cysteinyl-D-*O*-methythreonine is not turned over at all by IPNS (*43*), while the purely hydrocarbon "homologue" δ-(L-α-aminoadipoyl)-L-cysteinyl-D-isoleucine gives rise to a mixture of two β-lactam products (*44*−*46*). (Intriguingly, the epimeric δ-(L-α-aminoadipoyl)-L-cysteinyl-D-*O*-methy-*allo*-threonine *is* converted to a penam product by IPNS, but in relatively low yield (*43*); the corresponding D-*allo*-isoleucine analogue is also a substrate for the enzyme (*45*, *46*).)

The X-ray crystal structures reported herein reveal new binding modes and new metal-centered rearrangements in the IPNS active site, which demonstrate the delicate interplay of steric interactions and hydrophilic−hydrophobic effects around the catalytic iron center. Although the precise points at which the reactions of IPNS with ACG and ACA diverge from the path of reaction with the native substrate ACV remain uncertain, it is evident that the divergence is strongly influenced by differences in hydrophobicity and not simply due to differences in steric bulk.

ACKNOWLEDGMENT

We thank N. I. Burzlaff, C. M. H. Hensgens, K. Harlos, E. Garman, J. Keeping, J. Pitt, S. Lee, and the scientists at SRS Daresbury and ESRF Grenoble for help and discussions.

REFERENCES

1. Baldwin, J. E., and Schofield, C. J. (1992) The biosynthesis of β-lactams, in *The Chemistry of β-Lactams* (Page, M. I., Ed.) pp 1−78, Blackie, Glasgow, U.K.
2. Baldwin, J. E. (1985) Recent advances in the chemistry of the β-lactam antibiotics, in *Special Publication No. 52* (Brown, A. G., and Roberts, S. M., Eds.) pp 62−85, The Royal Society of Chemistry, London.
3. Baldwin, J. E., and Bradley, M. (1990) Isopenicillin N synthase: mechanistic studies, *Chem. Rev. 90*, 1079−1088.
4. Roach, P. L., Clifton, I. J., Hensgens, C. M. H., Shibata, N., Schofield, C. J., Hadju, J., and Baldwin, J. E. (1997) Structure of isopenicillin N synthase complexed with substrate and the mechanism of penicillin formation, *Nature 387*, 827−830.
5. Burzlaff, N. I., Rutledge, P. J., Clifton, I. J., Hensgens, C. M. H., Pickford, M., Adlington, R. M., Roach, P. L., and Baldwin, J. E. (1999) The reaction cycle of isopenicillin N synthase observed by X-ray diffraction, *Nature 401*, 721−724.
6. Baldwin, J. E., Bradley, M., Adlington, R. M., Norris, W. J., and Turner, N. J. (1991) Further evidence for the involvement of a monocyclic β-lactam in the enzymatic conversion of δ-L-α-aminoadipoyl-L-cysteinyl-D-valine into isopenicillin N, *Tetrahedron 47*, 457−480.
7. Costas, M., Mehn, M. P., Jensen, M. P., and Que, L. (2004) Dioxygen activation at mononuclear nonheme iron active sites: enzymes, models, and intermediates, *Chem. Rev. 104*, 939−986.
8. Hausinger, R. P. (2004) Fe(II)/alpha-ketoglutarate-dependent hydroxylases and related enzymes, *Crit. Rev. Biochem. Mol. Biol. 39*, 21−68.
9. Schofield, C. J., and Zhang, Z. H. (1999) Structural and mechanistic studies on 2-oxoglutarate-dependent oxygenases and related enzymes, *Curr. Opin. Struct. Biol. 9*, 722−731.
10. Lee, H. J., Lloyd, M. D., Clifton, I. J., Harlos, K., Dubus, A., Baldwin, J. E., Frere, J. M., and Schofield, C. J. (2001) Alteration of the co-substrate selectivity of deacetoxycephalosporin G synthase—The role of arginine 258, *J. Biol. Chem. 276*, 18290−18295.
11. Baldwin, J. E., Abraham, E. P., Lovel, C. G., and Ting, H.-H. (1984) Inhibition of penicillin biosynthesis by δ-(L-α-amino-δ-adipyl)-L-cysteinylglycine. Evidence for initial β-lactam ring formation, *J. Chem. Soc., Chem. Commun.*, 902−903.
12. Graf, P. (1986) Ph.D. Thesis, Eidgenössischen Technischen Hochschule, Zürich.
13. Sami, M., Brown, T. J. N., Roach, P. L., Schofield, C. J., and Baldwin, J. E. (1997) Glutamine-330 is not essential for activity in isopenicillin N synthase from *Aspergillus nidulans*, *FEBS Lett. 405*, 191−194.
14. Baldwin, J. E., Blackburn, J. M., Sutherland, J. D., and Wright, M. C. (1991) High-level soluble expression of isopenicillin N synthase isozymes in *E. coli*, *Tetrahedron 47*, 5991−6002.
15. Baldwin, J. E., Adlington, R. M., Domayne-Hayman, B. P., Knight, G., and Ting, H.-H. (1987) Use of the cyclopropylcarbinyl test to detect a radical-like intermediate in penicillin biosynthesis, *J. Chem. Soc., Chem. Commun.*, 1661−1663.
16. Baldwin, J. E., Abraham, E. P., Adlington, R. M., Murphy, J. A., Green, N. B., Ting, H.-H., and Usher, J. J. (1983) Penicillin biosynthesis. On the stereochemistry of carbon-sulphur bond formation with modified substrates, *J. Chem. Soc., Chem. Commun.*, 1319−1320.
17. Roach, P. L., Clifton, I. J., Fulop, V., Harlos, K., Barton, G. J., Hajdu, J., Andersson, I., Schofield, C. J., and Baldwin, J. E. (1995) Crystal structure of isopenicillin N synthase is the first from a new structural family of enzymes, *Nature 375*, 700−704.
18. Baldwin, J. E., Herchen, S. R., Johnson, B. L., Jung, M., Usher, J. J., and Wan, T. (1981) Synthesis of ACV and some carbon-13 and nitrogen-15 labelled isotopomers, *J. Chem. Soc., Perkin Trans. 1*, 2253−2257.
19. Bodanzky, M., and Bodanzky, A. (1984) The practice of peptide synthesis, in *Reactivity and Structure Concepts in Organic Chemistry* (Hafner, K., Rees, C. W., Trost, B. M., Lehn, J. M., Schleyer, R. V. R., and Zahruchik, R., Eds.), Springer-Verlag, Berlin, Germany.
20. Sheehan, J. C., Preston, J., and Cruickshank, P. A. (1965) A rapid synthesis of oligopeptide derivatives without isolation of intermediates, *J. Am. Chem. Soc. 87*, 2492−2493.
21. Wolfe, S., and Jokinen, M. G. (1979) Total synthesis of δ-(L-α-aminoadipoyl)-L-cysteinyl-D-valine (ACV), a biosynthetic precursor of penicillins and cephalosporins, *Can. J. Chem. 57*, 1388−1396.
22. Roach, P. L., Clifton, I. J., Hensgens, C. M. H., Shibata, N., Long, A. J., Strange, R. W., Hasnain, S. S., Schofield, C. J., Baldwin, J. E., and Hajdu, J. (1996) Anaerobic crystallisation of an isopenicillin N synthase•Fe(II)•substrate complex demonstrated by X-ray studies, *Eur. J. Biochem. 242*, 736−740.
23. Otwinowski, Z., and Minor, W. (1997) Processing of X-ray diffraction data collected in oscillation mode, *Methods Enzymol. 276*, 307−326.
24. Leslie, A. G. W. (1999) Integration of maromolecular diffraction data, *Acta Crystallogr., Sect. D 55*, 1696−1702.
25. Collaborative Computational Project, Number 4 (1994) The CCP4 suite: programs for protein crystallography, *Acta Crystallogr., Sect. D 50*, 760−763.
26. Brünger, A. T., Kuriyan, J., and Karplus, M. (1987) Crystallographic R-factor refinement by molecular-dynamics, *Science 235*, 458−460.
27. Sheldrick, G. M., and Schneider, T. R. (1997) SHELXL: high-resolution refinement, *Methods Enzymol. 277*, 319−343.
28. Jones, T. A., Zou, J. Y., Cowan, S. W., and Kjelgaard, M. (1991) Improved methods for building protein models in electron density maps and the location of errors in these models, *Acta Crystallogr.. Sect. A 47*, 110−119.
29. Kraulis, P. J. (1991) Molscript—A program to produce both detailed and schematic plots of protein structures, *J. Appl. Crystallogr. 24*, 946−950.
30. Esnouf, R. M. (1999) Further additions to MolScript version 1.4, including reading and contouring of electron-density maps, *Acta Crystallogr., Sect. D 55*, 938−940.
31. Merritt, E. A., and Bacon, D. J. (1997) Raster3D: photorealistic molecular graphics, *Methods Enzymol. 277*, 505−524.
32. Hegg, E. L., and Que, L., Jr. (1997) The 2-His-1-carboxylate facial triad—an emerging structural motif in mononuclear non-heme iron-(II) enzymes, *Eur. J. Biochem. 250*, 625−629.
33. Zhang, Z., Ren, J. S., Stammers, D. K., Baldwin, J. E., Harlos, K., and Schofield, C. J. (1999) Structural origins of the selectivity of the trifunctional oxygenase clavaminic acid synthase, *Nat. Struct. Biol. 7*, 127−133.
34. Zhou, J., Gunsior, M., Bachmann, B. O., Townsend, C. A., and Solomon, E. I. (1998) Substrate binding to the alpha-ketoglutarate-dependent non-heme iron enzyme clavaminate synthase 2: coupling mechanism of oxidative decarboxylation and hydroxylation, *J. Am. Chem. Soc. 120*, 13539−13540.
35. Zhou, J., Kelly, W. L., Bachmann, B. O., Gunsior, M., Townsend, C. A., and Solomon, E. I. (2001) Spectroscopic studies of substrate interactions with clavaminate synthase 2, a multifunctional alpha-KG-dependent non-heme iron enzyme: correlation with mechanisms and reactivities, *J. Am. Chem. Soc. 123*, 7388−7398.
36. Zhang, Z. H., Ren, J. S., Harlos, K., McKinnon, C. H., Clifton, I. J., and Schofield, C. J. (2002) Crystal structure of a clavaminate synthase-Fe(II)-2-oxoglutarate-substrate-NO complex: evidence for metal centred rearrangements, *FEBS Lett. 517*, 7−12.
37. Price, J. C., Barr, E. W., Tirupati, B., Bollinger, J. M., and Krebs, C. (2003) The first direct characterization of a high-valent iron intermediate in the reaction of an alpha-ketoglutarate-dependent dioxygenase: a high-spin Fe(IV) complex in taurine/alpha-ketoglutarate dioxygenase (TauD) from *Escherichia coli*, *Biochemistry 42*, 7497−7508.
38. Riggs-Gelasco, P. J., Price, J. C., Guyer, R. B., Brehm, J. H., Barr, E. W., Bollinger, J. M., and Krebs, C. (2004) EXAFS spectroscopic evidence for an Fe=O unit in the Fe(IV) intermediate observed during oxygen activation by taurine:alpha-ketoglutarate dioxygenase, *J. Am. Chem. Soc. 126*, 8108−8109.
39. Proshlyakov, D. A., Henshaw, T. F., Monterosso, G. R., Ryle, M. J., and Hausinger, R. P. (2004) Direct detection of oxygen intermediates in the non-heme Fe enzyme taurine/alpha-ketoglutarate dioxygenase, *J. Am. Chem. Soc. 126*, 1022−1023.
40. Abraham, E. P., Adlington, R. M., Baldwin, J. E., Crimmin, M. J., Field, L. D., Jayatilake, G. S., and White, R. L. (1982) Monocyclic β-lactam tripeptide 1-(D-carboxy-2-methylpropyl)-3-L-(δ-L-2-aminoadipamido)-4-L-mercaptoazetidin-2-one, a putative

intermediate in penicillin biosynthesis, *J. Chem. Soc., Chem. Commun.*, 1130−1132.
41. Baldwin, J. E., Abraham, E. P., Adlington, R. M., Crimmin, M. J., Field, L. D., Jayatilake, G. S., White, R. L., and Usher, J. J. (1984) The synthesis and reactions of a monocyclic β-lactam tripeptide, 1-[(1*R*)-carboxy-2-methylpropyl]-(3*R*)-[(5*S*)-5-amino-5-carboxypentanamido]-(4*R*)-mercaptoazetidin-2-one, a putative intermediate in penicillin biosynthesis, *Tetrahedron 40*, 1907−1918.
42. Grummitt, A. R., Rutledge, P. J., Clifton, I. J., and Baldwin, J. E. (2004) Active-site-mediated elimination of hydrogen fluoride from a fluorinated substrate analogue by isopenicillin N synthase, *Biochem. J. 382*, 659−666.
43. Baldwin, J. E., Adlington, R. M., Basak, A., Flitsch, S. L., Petursson, S., Turner, N. J., and Ting, H.-H. (1986) Enzymatic synthesis of a new type of penicillin, *J. Chem. Soc., Chem. Commun.*, 975−976.
44. Bahadur, G., Baldwin, J. E., Field, L. D., Lehtonen, E.-M. M., Usher, J. J., Vallejo, C. A., Abraham, E. P., and White, R. L. (1981) Direct ^{1}H NMR observation of the cell-free conversion of δ-(L-α-aminoadipyl)-L-cysteinyl-D-valine and δ-(L-α-aminoadipyl)-L-cysteinyl-D-(−)-isoleucine into penicillins, *J. Chem. Soc., Chem. Commun.*, 917−919.
45. Bahadur, G. A., Baldwin, J. E., Usher, J. J., Abraham, E. P., Jayatilake, G. S., and White, R. L. (1981) Cell-free biosynthesis of penicillins. Conversion of peptides into new β-lactam antibiotics, *J. Am. Chem. Soc. 103*, 7650−7651.
46. Baldwin, J. E., Adlington, R. M., Turner, N. J., Domayne-Hayman, B. P., Ting, H.-H., Derome, A. E., and Murphy, J. A. (1984) Penicillin biosynthesis: enzymatic synthesis of new cephams, *J. Chem. Soc., Chem. Commun.*, 1167−1170.

BI047478Q